International Journal of Energy
ISSN: 2957-9473 | Vol. 2, No. 3, 2023

Comparison of Change in Nanopore Structure of Oil Shale after Anhydrous and Sub/Supercritical Water Pyrolysis

Yaolin Yang, Xianda Sun, Wei Li

College of Earth Sciences, Northeast Petroleum University, Daqing 163318, China

Abstract: Oil shale is an important part of unconventional resources, which is considered as an important replacement for traditional oil resources. At present, the underground in-situ conversion method of oil shale is mainly aimed at shallow reservoirs, and it is difficult to apply to in-situ exploitation of oil shale with a depth of more than 1000m. In view of the portability, fracturing and extraction characteristics of high-pressure sub/supercritical water, it has become the research direction of in-situ mining of deep oil shale. The evolution of pore structure of oil shale is the basis for exploring the production mechanism of sub/supercritical water pyrolysis of oil and gas, which has important theoretical and scientific significance for improving the development and utilization of in-situ injection of sub/supercritical water in deep oil shale. Therefore, in this paper, the oil shale of Jijuntun Formation of Paleogene in Fushun Basin is taken as the research object. The pyrolysis experiments of oil shale in three ways, namely, water-free (electric heating), subcritical water and supercritical water, are carried out by means of high temperature and high-pressure source rock pyrolysis simulation device. The evolution characteristics of nano-pore structure under different pyrolysis methods are studied by XRD and low temperature nitrogen adsorption technology. The results show that, compared with anhydrous pyrolysis at the same temperature, the pore size of 3-30 nm of oil shale increases significantly after sub/supercritical water pyrolysis. The phenomenon of kaolinite illite fossilization increases, and the overall weak acidic environment is more conducive to the transformation of illite into Illite and montmorillonite mixed layer minerals, easier to increase the pore space in oil shale, and conducive to the migration and accumulation of produced oil and gas.

Keywords: Oil Shale; Sub/Supercritical Water Pyrolysis; Pore Structure.

1. Introduction

In recent years, influenced by economic development, China's energy consumption is increasing day by day, and the dependence of petroleum on foreign countries is rising year after year. Energy security has attracted much attention. China's unconventional oil and gas resources have huge potential and abundant reserves, which are strategic replacement resources for future energy development. As an important part of unconventional energy, oil shale is a strategic reserve resource and supplementary energy. The development and utilization of oil shale is of great significance for optimizing China's energy structure and ensuring our energy security. Limited by technical and economic conditions, oil shale resources are slowly exploited with low recovery rate, and most of the exploitation is only aimed at shallow reservoirs. To find a more appropriate way of recovery, reasonable exploitation of resources with too deep burial and too much reservoir stress can effectively alleviate the current production situation of excess demand and poor production [1-4].

The results show that a large number of pore structures of different sizes appear after coal is extracted and pyrolyzed by supercritical water, which indicates that supercritical water can reform the solid skeleton of organic rock to a certain extent and improve its permeability [5]. In view of the portability, solubility, cracking and extraction characteristics of high-pressure subcritical water and supercritical water [6], the selection of subcritical water and supercritical water as injection fluids has become a new research direction for in-situ mining of deep oil shale. Yanik [7] and harfi [8] carried out pyrolysis extraction experiments on oil shale in Turkey and Morocco respectively in supercritical water (400℃, 25MPa) environment, and found that the use of supercritical water can increase the internal porosity of shale, and oil and gas production increased by about 16%. Kang [9] exploited shale gas reservoirs by using supercritical water fracturing, and found that the permeability of shale increased by 197.06 times and the porosity increased by 1.66 times. The study showed that the dissolution decomposition of minerals made the nanoscale pores more complex, increased the porosity of fracture network in shale, and led to the enhancement of natural gas transportation capacity. Meng [10] used supercritical water to pyrolyze organic rich shale and analyzed its products and distribution characteristics. The study found that the production of shale oil increased at a rate of twice as fast as the temperature increased between 385℃ and 425℃. The intermediate hot bitumen retained in the core generated by kerogen pyrolysis continues to decompose with the increase of temperature, and a large number of pores are formed in the core matrix. Kang [11] treated the fracked shale with supercritical water and found that the porosity and permeability of the shale increased by 213.43% and 2198.37%, respectively. Further studies found that the mechanisms affecting pore structure and mineral composition include oxidation-catalyzed decomposition of organic matter and reducing minerals, acid-catalyzed decomposition of carbonate and feldspar minerals, fracture propagation caused by hydrothermal catalysis, and fracture extension caused by cementation weakening.

The above results confirm that it is feasible to use subcritical water and supercritical water as pyrolysis medium for in-situ transformation of oil shale, but the changes of nano-pore structure in oil shale after pyrolysis have not been

studied. On the basis of previous experiments, the evolution characteristics of nanopore structure of oil shale after near critical water/supercritical water pyrolysis were further studied in this paper.

2. Samples and Experiments

In this paper, the samples were taken from the oil shale of the Paleogene Jijuntun Formation rich deposit in Fushun Basin. The depth of the samples is about 200m. The color of the samples is dark brown, showing weak grease luster. The oil content level is medium, about 5.59%. T_{max} is 434℃ and R_o is 0.49. In summary, the Fushun oil shale samples belong to immature source rocks, which are in the early stage of the oil generation window and have high oil generation potential.

2.1. Sample Preparation

The samples were collected and crushed and screened. Six irregular bulk samples smaller than 2cm (about 20g each) were selected. The pyrolysis experiments of the above samples were carried out in anhydrous (electric heating), subcritical water and supercritical water environments using the DK-III pore pressure simulation experiment instrument for hydrocarbon generation and expulsion. The constant temperature time was 48h for all of the samples. The specific parameters were set in the following table (Table 1).

Table 1. Parameters of reaction conditions under different pyrolysis environments

Pyrolysis environment	Sample number	Experimental temperature (° C)	Experimental pressure (MPa)	Sample weight (g)	Amount of water added (ml)
Electric heating	An-300	300	0.32	59.62	0
	An-360	360	1.31	60.02	0
	An-450	450	5.44	60.30	0
Subcritical water	CW-300	300	10	59.43	30
	CW-360	360	20	60.27	30
Supercritical water	SW-450	450	27	61.2	30

First, the oil shale is loaded into the high-temperature and high-pressure reactor, and the reactor is installed on the test bench. After pressurization and sealing, the inert gas of 5 ~ 10MPa is injected into the reactor, and the leakage test is static. After no leakage, the gas is released; Then, use a vacuum pump to vacuum the reactor before inflating it, repeat 3 to 5 times to ensure that the reactor is vacuum. Then, a high-pressure pump is used to inject 30ml pure water into the reactor (electric heating does not require injection) to ensure that the oil shale sample is in full contact with water to ensure that the sample is pyrolyzed in a complete sub/supercritical water environment. In order to ensure the hydrocarbon generation reaction and hydrocarbon expulsion process of oil shale samples in sub/supercritical water environment, and keep the fluid pressure constant in the experimental system, let the subcritical water to drink supercritical water fill the pore space of oil shale samples, oil shale samples in the process of water absorption will make the fluid pressure in the system drop, when the pressure in the system is constant and no longer drops, Indicating that the pores of the oil shale sample have been filled with water. According to the temperature and pressure parameters in the table, open the heating switch of the experimental device, and the heating rate of the heating chamber is set to 1℃/min. After reaching the set final temperature, the constant temperature is 48h. The fluid pressure in the experiment process is completely generated by hydrocarbon generation and supercharging. After the pyrolysis simulation experiment reaches the predetermined 48h, wait for the temperature to drop to 180℃, connect the product collection device, open the hydrocarbon exhaust valve, discharge the oil and gas products, collect the condensate oil discharged with the gas through the cold trap, and collect the gas through the metering pipe and measure its volume. Finally, after waiting for the whole reactor to drop to room temperature, the oil shale sample residue is removed, and the oil attached to the reactor and the pipeline is cleaned with methylene chloride, and the collected mixture is further analyzed.

3. Analysis of Results

3.1. XRD Mineral Analysis under Different Pyrolysis Modes

There are many kinds of minerals in oil shale, and the different kinds and contents of minerals will affect the absorption and reflection effect of X-ray. Therefore, XRD mineral composition analysis was carried out on Fushun oil shale samples at different temperatures under two pyrolysis methods. The mineral composition of Fushun oil shale is listed in Table 2. According to the XRD test results, the XRD comparison patterns of anhydrous pyrolysis samples, sub/supercritical water pyrolysis samples and original samples of oil shale at 300℃, 360℃ and 450℃ were drawn respectively, as shown in Figure 1.

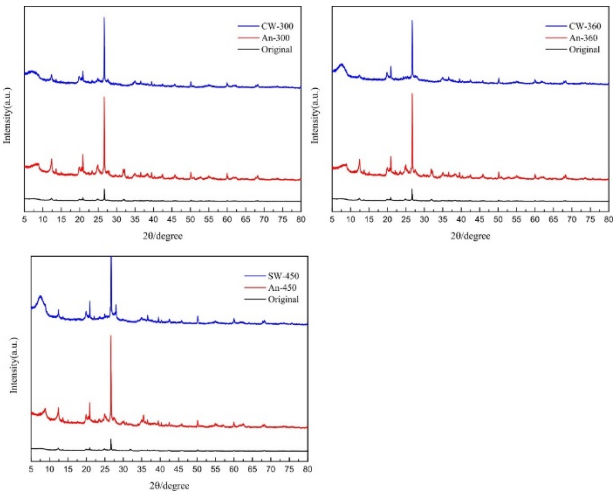


Fig 1. XRD patterns of Fushun oil shale samples at different temperatures

From the data in Table 2 and Figure 1, it can be seen that the main mineral components of Fushun oil shale are quartz and clay minerals, with a small amount of potassium feldspar, plagioclase, siderite and pyrite. The clay minerals mainly include kaolinite and illite. The XRD pattern shows that the main mineral compositions of oil shale samples have not

changed basically, and the variation intensity of each phase type and diffraction peak is not big. It indicates that the chemical properties of the main mineral composition of the sample are relatively stable.

Table 3 shows the relative content and mixed-layer ratio of clay minerals in the two pyrolysis methods at different temperatures. It can be clearly seen that: (1) With the increase of temperature, the content of Illite and montmorillonite mixed layer in the sub/supercritical water pyrolysis series increases significantly and is much higher than the original sample, while the anhydrous pyrolysis series shows a downward trend with the increase of temperature, which is lower than the original sample. The Illite and montmorillonite mixed layer ratio refers to the content ratio of illite and smectite in minerals. The increase of Illite and montmorillonite mixed layer is conducive to the increase of pore space in oil shale. (2) With the increase of temperature, the contents of illite and kaolinite in sub/supercritical water pyrolysis series are slightly lower than those in anhydrous pyrolysis series at the same temperature, and the relative contents of the two decreases with the increase of temperature.

Table 2. Mineral component contents of Fushun oil shale

Sample No.	Mineral content (%)					
	quartz	Potassium feldspar	plagioclase	siderite	pyrite	Clay minerals
As-is	28.3	2.6	1.4	14.7	0.9	52.1
An-300	29.2	2.0	3.1	12.3	1.0	52.4
An-360	31.5	3.0	2.0	12.1	1.0	50.4
An-450	36.1	3.6	1.7	/	/	58.6
CW-300	30.4	2.5	2.7	/	0.7	63.7
CW-360	32.9	2.9	5.3	/	/	57.0
SW-450	36.4	5.3	3.9	/	/	50.6

Table 3. Relative content and mixed layer ratio of clay minerals in Fushun oil shale samples at different temperatures

Sample No.	Relative clay mineral content (%)						Mixed layer ratio (%S)	
	S	I/S	It	Kao	C	C/S	I/S	C/S
As-is	/	59	9	32	/	/	40	/
An-300	/	48	13	39	/	/	20	/
An-360	/	39	25	36	/	/	20	/
An-450	/	38	28	34	/	/	15	/
CW-300	/	69	10	21	/	/	45	/
CW-360	/	83	7	10	/	/	45	/
SW-450	/	88	8	4	/	/	25	/

Note: S- smectites; I/ S-illite and montmorillonite mixed layer; I-illite; K-kaolinite; C-chlorite; C/S- green mixed layer

3.2. Low-temperature N Adsorption Characterization2 of Nanopore Structure

Low-temperature N_2 adsorption experiments were carried out on oil shale samples from two pyrolysis methods at different temperatures to characterize the evolution of nanopore structure of oil shale before and after pyrolysis. In order to eliminate interference factors such as residual liquid hydrocarbons [12] chloroform was used to extract oil shale samples. FIG. 2 shows the low-temperature N_2 adsorption isotherm of the sample after the chloroform extraction was advanced. According to the previous classification [13], the adsorption isotherms of the samples were all type IV isotherms, and the isotherm types did not change significantly with the increase of temperature. Due to capillary condensation of mesopore and macropore, all oil shale samples have an obvious inflection point near the relative partial pressure $P/P_0 = 0.5$ after the advance of chloroform extraction, resulting in adsorption hysteresis rings. According to the characteristics of the hysteresis ring, the type of the hysteresis ring can be determined, and then the pore shape can be determined. The use of chloroform extraction can remove the interference of incomplete pyrolysis residual oil factors, and better determine the pore structure type.

For the anhydrous heating series: in the case of chloroform extraction advance, An-360 is the cylindrical pore of H1 type hysterecyclic ring, and An-300 and An-450 are the wide slit pore of H3 type hysterecyclic ring. The pore type changes from slit to cylinder to slit, which may be related to the occurrence of residual oil. After chloroform extraction, the three samples all showed wide slit pores of H3 type hystere-ring, among which An-300 and An-360 hystere-ring significantly increased, and the proportion of wide slit pores increased. After extraction of An-360, the pore type changed from cylindrical to slit, indicating that the residual oil in the sample mainly exists in the slit pores. At 450℃, oil shale is mainly gas, so after the advance of chloroform extraction, the N-adsorption curve$_2$ of An-450 basically coincides.

For the sub/supercritical water heating series, CW-300, CW-360 and SW-450 all have wide slit pores of H3 hysterical ring after the early extraction of chloroform. After chloroform extraction, the pore types of the three samples did not change, but the hysteric rings of CW-300 and CW-360 significantly increased, indicating that the proportion of wide slit pores increased. At 450℃, oil shale is mainly gassing generation, so the N adsorption$_2$ curve of SW-450 basically coincides

after the advance of chloroform extraction. Compared with the anhydrous pyrolysis series at the same temperature, the hysteresis rings of sub/supercritical water pyrolysis series increase significantly, indicating that the sub/supercritical water environment promotes the formation of slit pores of oil shale.

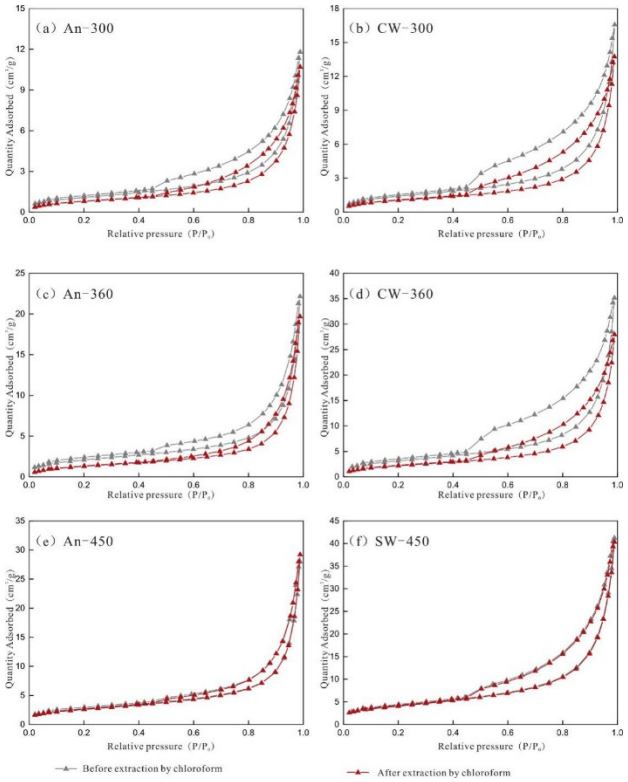


Fig 2. Comparison of low-temperature N_2 adsorption isotherms after chloroform extraction

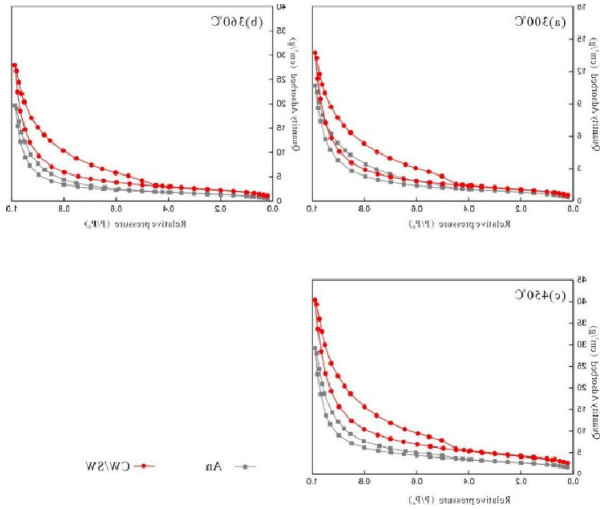


Fig 3. Comparison of low-temperature N_2 adsorption isotherms and temperature before chloroform extraction

FIG. 3 is a comparison of the N-$_2$adsorption isotherms of the two pyrolysis methods at the same temperature before chloroform extraction. It can be seen from the figure that, with the increase of temperature, the hysteric ring of anhydrous pyrolysis series is weakened, indicating that the proportion of slit pores transforming into cylindrical pores in oil shale increases under anhydrous environment. The hysteresis rings of sub/supercritical water pyrolysis series increase, indicating that the sub/supercritical water environment promotes the generation of slit pores in oil shale. By contrast, there are differences between the two pyrolysis methods in the change of nanopore structure. Near-supercritical water pyrolysis environment is more conducive to the formation of slit pores. On the other hand, at the same temperature, the hysteresis rings of sub/supercritical water pyrolysis series are significantly larger than those of anhydrous pyrolysis series, indicating that the number of nanopores of oil shale increases in sub/supercritical water environment.

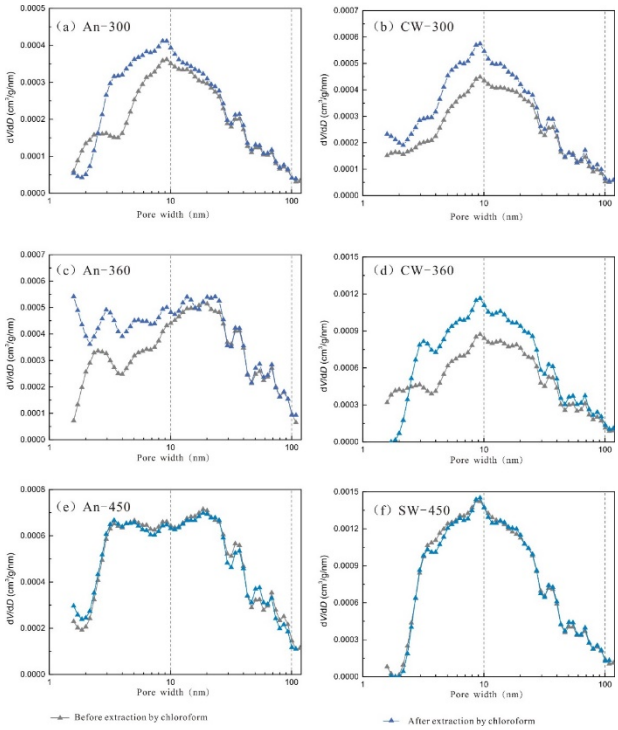


Fig 4. Comparison of N-$_2$pore size distribution characteristics at low temperature after chloroform extraction in advance

Figure 4 shows the pore size distribution of two pyrolysis methods after chloroform extraction advance. The pore evolution characteristics of oil shale under different pyrolysis methods can be more clearly analyzed by using the pore distribution diagram.

For anhydrous pyrolysis series, the pore size distribution is multi-peak type. The pore size distribution is similar at 300℃ and 360℃, and the pore volume increases slightly. At 450℃, the mesoporous pore size was evenly distributed between 3-30nm, and the number of pores increased significantly. After chloroform extraction, at 300℃, the number of micropores was less, and the number of mesoporous pores increased at 2-10nm. At 360℃, the number of micropores at about 2 nm increased greatly, and the mesoporous volume was about twice of the extraction advance. After 450℃ extraction advances, the curves basically coincide, and the mesopore volume is slightly lower than the extraction advance. Explanation: With the increase of temperature, the distribution of pore size in oil shale in anhydrous environment increases slightly, and the number of pores increases. Most of the retained liquid hydrocarbons exist in the pores of 2-10 nm.

For the sub/supercritical water pyrolysis series, the pore size distribution is multi-peak type, and the pore size is about 10 nm. The pore size distribution of samples at three temperatures is basically the same. The pore size of samples at 360℃ is about twice of that at 300℃, and that at 450℃ is about three times of that at 300℃. After chloroform extraction, the number of micropores was significantly reduced and the number of mesoporous holes increased at

360℃. At 450℃, the pore size distribution curve basically coincides with that at 300℃, and the pore volume increases about three times. Explanation: With the increase of temperature, the pore volume and pore number of oil shale in sub/supercritical water environment increase by multiple times, and most of the retained liquid hydrocarbons exist in the pores at 2-30nm.

It can be found that: (1) Compared with the anhydrous pyrolysis series, the pore volume and number of the sub/supercritical water pyrolysis series increase significantly, and the pore size distribution is more concentrated, mostly about 10 nm mesoporous; (2) Residual oil mainly occurs in pores <30nm; (3) At 450℃, oil shale is mainly gassing generation, so the pore morphology changes little and the pore size distribution curve changes little.

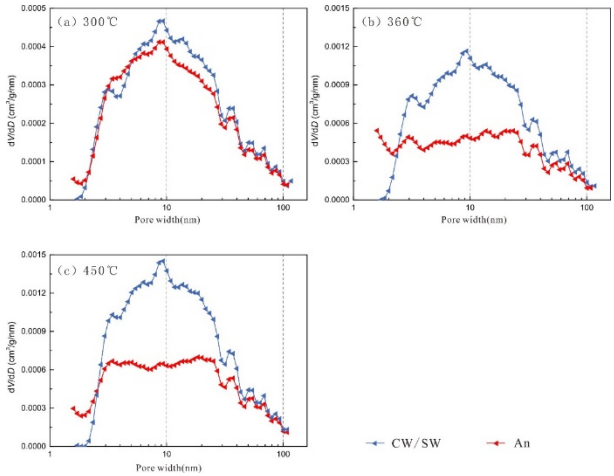


Fig 5. Comparison of pore size distribution of low-temperature N_2 adsorption after chloroform extraction with temperature

FIG. 5 is the comparison of pore size distribution of the two pyrolysis methods at the same temperature after chloroform extraction. From the perspective of pore diameter, at 300℃, the pore size distribution of anhydrous pyrolysis and subcritical water pyrolysis is basically the same, and the pore size is mostly concentrated around 10 nm. At 360℃, there is a large difference in pore size distribution between the two pyrolysis methods, and there is little difference in multi-peaks during anhydrous pyrolysis, and the number of micropores increases. The number of mesoporous pores during subcritical water pyrolysis at 3-30nm increases significantly, which is about twice of that at 300℃. In terms of pore volume, there is no significant difference between anhydrous pyrolysis and subcritical water pyrolysis at 300℃. At 360℃ and 450℃, the pore volume of sub/supercritical water pyrolysis is about twice that of anhydrous pyrolysis.

In general, the pore volume changes strongly at < 50 nm when the pyrolysis temperature is between 300℃ and 360℃; When the temperature is > 360℃, the < 100 nm pore changes significantly. This indicates that during the oil generation window period, most of the generated pores are < 50 nm, and during the gas generation window period, the variation range of pore size becomes wider.

Based on the N adsorption curve and pore size distribution diagram, the specific parameters of samples at different temperatures under the two pyrolysis methods are calculated in Table 4. $_2$Based on the analysis of the two data, it can be seen that: (1) the adsorption capacity, specific surface area and total pore volume of sub/supercritical water pyrolysis series are significantly higher than those of anhydrous pyrolysis series at the same temperature; The average pore size of anhydrous pyrolysis series is higher than that of sub/supercritical water pyrolysis series at the same temperature. This indicates that with the increase of temperature, the sub/supercritical water environment promotes the increase of pores in oil shale, especially the number of pores in supercritical water at 450℃ (SW-450) is the largest. Combined with the pore size distribution diagram, most of the increased pores are distributed between 3-30 nm. The anhydrous pyrolysis environment increases the proportion of micropores in oil shale, but the number of generated pores is small. (2) The specific surface area and total pore volume of An-300 and CW-300 decreased compared with the normal temperature, which could be attributed to the adsorption and plugging of residual oil. (3) At 300℃ to 360℃, the residual oil in the pores of pyrolized oil shale blocked part of the pores, reducing the pore volume of nano-sized pores. According to the pore size distribution diagram, most of the residual oil existed in pores < 30 nm.

Table 4. Summarizes the data of pore - macropore (2-200nm) specific surface and pore volume measurement

Sample Number	Adsorption amount (cm^3/g)		BET specific surface area (m^2/g)		Total pore volume (cm^3/g)		Average pore size (nm)	
	Before	After	Before	After	Before	After	Before	After
original	15.37	-	5.62	-	0.0238	-	9.66	-
An-300	10.69	11.80	3.02	3.97	0.0165	0.0183	13.89	11.64
An-360	19.69	22.29	4.93	7.94	0.0305	0.0345	18.15	14.35
An-450	29.20	27.99	9.37	9.87	0.0452	0.0433	15.77	15.40
CW-300	13.74	16.56	3.90	5.20	0.0213	0.0256	11.00	9.69
CW-360	27.96	35.15	8.19	11.51	0.0432	0.0544	11.87	9.44
SW-450	40.32	41.25	14.58	15.06	0.0624	0.0638	11.60	11.63

3.3. Influence of Sub/Supercritical Water Pyrolysis on the Evolution of Nanopore Structure of Oil Shale

In general, compared with anhydrous pyrolysis, the nano-pore structure in oil shale after sub/supercritical water pyrolysis at the same temperature is as follows: (1) With the increase of temperature, the pore volume and quantity in the range of 3-30 nm increase significantly, with the largest number of SW-450 pores. (2) During the oil generation window (300℃ -360 ℃), most of the generated pores are less than 50 nm. During the gas generation window (> 360℃), the pore size varies widely. (3) Sub/supercritical water pyrolysis improves the balance of porosity distribution in each pore segment to a certain extent, and the pore size distribution becomes wider. It also strengthens the correlation between pore groups of different pore sizes, enhances the pore connectivity inside the oil shale, forms a more developed pore network, and is easier to generate oil and gas migration and expulsion.

On the whole, the near-supercritical water environment has a great influence on the nano-structure of oil shale, and the change of chemical structure has a certain influence on the change of nano-pore structure. In order to explore the influence of chemical structure of mineral and organic matter on the evolution of nanopore structure, the relative content-pore volume relationship diagram of kaolinite (FIG. 6.a) and the relative content-pore volume relationship diagram of Imon mixed layer (FIG. 6.b) are drawn based on relevant data. The comparative findings are as follows:

(1) The Illite and montmorillonite mixed layer content and pore volume of the sub/supercritical water series show a significant positive correlation with temperature (FIG. 6.b), indicating that with the increase of temperature, the increase of Illite and montmorillonite mixed layer content leads to the increase of pore volume and the increase of mesoporous and macropore content in oil shale. Anhydrous pyrolysis series presents a negative correlation change, that is, with the increase of temperature, the content of illite and montmorillonite mixed layer decreases and the pore volume increases slightly. Combined with the change of pore size distribution of anhydrous pyrolysis series, it indicates that the content of Illite and montmorillonite mixed layer in clay minerals affects the content of intermediate pore and macropore in oil shale. The increase of Leimon mixed layer content in sub/supercritical water system may also be related to the sub/supercritical water environment itself.

It is generally believed that the dissolution of feldspar provides most of the aluminum, silicon and oxygen formed by kaolinite. The high temperature and high-pressure environment promote the dissolution of potassium feldspar, which is conducive to the formation of kaolinite. When the concentration of H^+ in the environment decreases and the concentration of alkaline ions such as K^+ and Na^+ rises, the stability of kaolinite itself begins to decline. With the dissolution of potassium feldspar, the ratio of K^+/H^+ in the solution gradually increases, reaching the two-phase boundary of kaolinite and illite, and the rapid occurrence of kaolinite illite, the threshold temperature is about 120-140 ℃ [14,15]. It is found that: in the weak acidic environment, illite is easy to undergo weak hydrolysis and further transform into Amon mixed layer minerals [16]. Under the condition of high temperature and high pressure, due to the increase of water ion product, the supercritical water has the function of acid catalyst, and its existence environment is weak acidic environment [17]. As can be seen from Figure 6, the kaolinite content decreases as the temperature increases, and the pore volume is negatively correlated with the content of kaolinite (Figure 6.a). The content of anhydrous series has a small variation range, while the remaining content of kaolinite is high, indicating that the reaction of kaolinite illitalization is relatively small in anhydrous environment, which further affects the content of illite and montmorillonite mixed layer (Figure 6.b). In the sub/supercritical water environment, the phenomenon of kaolinite illitalization increases, and the overall weak acidic environment is more beneficial to the transformation of illite into illite and montmorillonite mixed layer minerals, and easier to increase the pore space in oil shale. By comparing the changes of relative contents of kaolinite and Illite and montmorillonite mixed layer in the two pyrolysis methods before and after pyrolysis (FIG. 6.c, d, e, f), it is found that the slope of 360-450 ℃ is significantly higher than that of 300-360 ℃, indicating that most of the drastic changes in internal structure of oil shale caused by pyrolysis occur after 360℃.

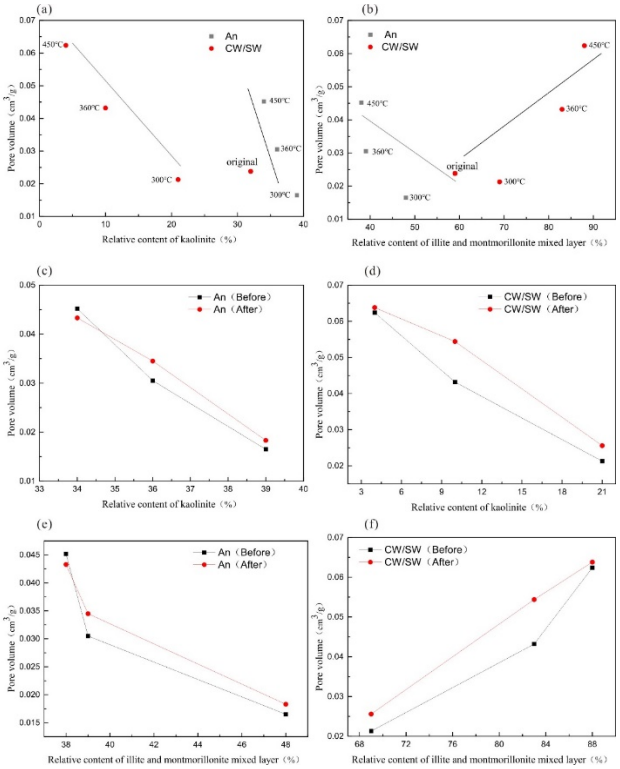


Fig 6. Relation between relative content of Kaolinite and Illite and montmorillonite mixed layer and pore volume

4. Conclusion

In this paper, high-temperature and high-pressure pyrolysis simulation experiments are used to systematically study the effects of anhydrous (electric heating), subcritical water and supercritical water pyrolysis on the nanopore structure of oil shale. The main research conclusions are as follows:

(1) The evolution law of nano-pore structure in the range of 2-200nm was explored through the low-temperature N adsorption experiment of samples after chloroform extraction. $_2$The specific results are as follows: (1) At 300℃ to 360℃, residual oil in the pores of pyrolyzed oil shale blocked part of the pores, reducing the pore volume of nano-sized pores, and most of the residual oil existed in pores < 30 nm; (2) Compared with anhydrous pyrolysis, at the same temperature, the internal pores of oil shale after sub/supercritical water pyrolysis increase a lot, and SW-450 pores are the most abundant, and most of the increased pores are distributed between 3-30 nm.

(2) In sub/supercritical water pyrolysis mode, the evolution characteristics of nano-pore structure are controlled by inorganic minerals of oil shale. Compared with anhydrous pyrolysis, in the sub/supercritical water environment at the same temperature, the illinization of kaolinite increases, and the overall weak acidic environment is more beneficial to the transformation of illite into Illite and montmorillonite mixed layer minerals, and easier to increase the pore space in oil shale.

References

[1] Ministry of Natural Resources of the People's Republic of China. China Mineral Resources Report 2021 [M]. Beijing: Geological Publishing House, 2021.

[2] Deng Sunhua. Study on extraction of organic matter from massive oil shale by near-critical water [D]. Changchun: Jilin University, 2013.

[3] Hou Jili, Ma Yue, Li Shuyuan, et al. Development and utilization of oil shale resources in the world [J]. Progress in Chemical Industry, 2015, 34: 1183-1190.

[4] Liu Zhaojun, Dong Qingshui, Ye Songqing, et al. Current situation of oil shale resources in China [J]. Journal of Jilin University (Earth Science Edition), 2006:869-876.

[5] Xue Jinxia, Liu Zhonghua, Yang Dong, et al. Experimental study on the transformation of low permeability coal by supercritical water pumping [J]. Science and Technology Information Development and Economy, 2007:178-180.

[6] Zheng Lan, Chen Kaixun. Research and application status of super (near) critical water [J]. Petrochemical Industry, 2012, 41: 621-629.

[7] harfi K E, Bennouna C, Mokhlisse A, et al. Supercritical fluid extraction of Moroccan (Timahdit) oil shale with water [J]. Journal of Analytical and Applied Pyrolysis, 1999.

[8] Yanik J, Yuksel M, Salam M, et al. Characterization of the oil fractions of shale oil obtained by pyrolysis and supercritical water extraction [J]. Fuel, 1995, 74(1): 46-50.

[9] Kang Y, Li P, Chen M, et al. Enhancing porosity and permeability of shale matrix through supercritical water treatment [J]. Journal of Natural Gas Science and Engineering, 2022, 101: 104530.

[10] Meng F, Yao C, Zhang H,et al. Experimental Investigation on the Pyrolysis Process and Product Distribution Characteristics of Organic-Rich Shale Via Supercritical Water [J]. SSRN Electronic Journal, 2022.

[11] Kang Y, Li P, Cao W, et al. Investigation of pore structure alteration and permeability enhancement of shale matrix by supercritical water treatment after hydraulic fracturing [J]. Petroleum, 2022.

[12] Caniego F J, Mart M A, Jose F. Renyi dimensions of soil pore size distribution [J]. 2003, 112(3-4): 0-216.

[13] Riedi R H, Crouse M S. A multifractal wavelet model with application to network traffic [J]. IEEE Transactions on Information Theory, 1999, 45(3): 992-1018.

[14] Cai Laixing, Yang Tian, Tian Jingchun, et al. Development characteristics and growth mechanism of clay minerals in tight sandstone reservoirs [J]. Acta Sedimentologica Sinica: 1-44.

[15] Huang Sijing, Sun Wei, Huang Peipei, et al. Formation mechanism of authigenic illite in clastic rocks of Taiyuan Formation, eastern Ordos Basin and its influence on reservoir formation [J]. Journal of Mineralogy and Petrology, 2009, 29: 25-32.

[16] Zhang Na. Mineralogical characteristics of seabed sediments in Beibu Gulf and their response to environment [D]. Beijing: China University of Geosciences (Beijing), 2015.

[17] Zheng Lan, Chen Kaixun. Research and application status of super (near) critical water [J]. Petrochemical Industry, 2012, 41(6): 9. (in Chinese)